The reorganization and reactivation of hippocampal maps predict spatial memory performance

David Dupret, Joseph O'Neill, Barty Pleydell-Bouverie and Jozsef Csicsvari

MRC Anatomical Neuropharmacology Unit, Department of Pharmacology, University of Oxford, Mansfield Road, Oxford OX1 3TH, United Kingdom

Supplementary Information

1. Supplementary Discussion

In this study, we present evidence that support the hypothesis that the reorganization, reactivation and reinstatement of hippocampal firing patterns represent the formation and expression of spatial memory traces. However, an alternative hypothesis suggests that hippocampal representations reflect the spatial distribution of attention in the environment, meaning that goal-oriented remapping could relate to increased attention at goal locations, rather than mnemonic processes *per se*. In order to explain a correlation between goal-oriented reorganization of hippocampal network activity and the future memory performance of the animal (as in our data), this view argues that attention levels present at each location must not only govern the degree of place cell reorganization, but must also direct the later behavior of the animal. In this study we show that hippocampal representations present at the end of the learning session recur later during the post-probe exploration. Given that the "attentional hypothesis" assumes that attention will govern remapping independently in different sessions, the recurrence of representations could be only explained if one assumes identical distribution of spatial attention levels in learning and post-probe sessions. This is unlikely; particularly if one considers that no food reward

Nature Neuroscience: doi:10.1038/nn.2599

was given in the post-probe session. However an alternative scenario is possible in which attention to distal spatial cues at goal locations may drive place cell reorganization during the learning session only. Yet it is not clear in this case why attentional modulation would take place during learning only, considering that spatial attention to distal cues is needed to perform the probe test. Moreover, even in this latter case, place maps, including the goal-oriented maps observed here, are expected to contribute to spatial memory performance by the means of supporting efficient navigation to goal locations. Therefore, the fact that we see similar goal-related representations during recall to those during learning ought to result from something learned, even if the learning process itself involved attention. Moreover, the "attentional hypothesis" would also require that attention at goal locations determine the strength of the reactivation of goal-related patterns when the rat was resting in the start-box at times beyond the learning period. Therefore, the memory performance-linked reorganization and reactivation of hippocampal firing patterns described in our study are most likely to have functional consequences in spatial memory process. Accordingly, the most parsimonious explanation of such reorganization, reactivation and reinstatement of hippocampal neuronal activity points to a role in the encoding, storage and retrieval of spatial memory.

Nature Neuroscience: doi:10.1038/nn.2599

2. Supplementary Methods

Subjects. All procedures were carried out in accordance with the Animals (Scientific Procedures) Act, 1986 (UK) and associated procedures under an approved project license. A total of seven adult male Long-Evans rats (Harlan, UK) were used for the experiments. Rats were housed individually in standard rodent cages (56×40×26 cm) in a temperature and humidity controlled animal room. All rats were maintained on a 12 hr light/dark cycle and all testing performed during the light phase. Food and water were available *ad libitum* prior to the recording procedures and body weight at the time of surgery was 350-400 g.

Surgery and data acquisition. The surgical and recording procedures, electrode preparation, implantation and spike sorting methods have been described before [1,2]. In short, rats were implanted with 16 independently movable wire-tetrodes under deep anesthesia using isoflurane (0.5-2 %), oxygen (2 l/min) and an initial dose of buprenorphine (0.1 mg/kg). Wire tetrodes constructed from 12 μm diameter tungsten wires (H-Formvar insulation with Butyral bond coat, California Fine Wire, Grover Beach CA) were attached to the microdrives, enabling their independent movement. The tetrode tips were gold-plated to reduce electrode impedances to 250-500 kΩ. During surgery a craniotomy was performed above the right dorsal portion of the hippocampus, centered at AP=-3.8; ML=2.5, the dura mater removed and the electrode bundles implanted into the superficial layers of the neocortex, after which both the exposed cortex and the electrode shanks were sealed with paraffin wax. Two micro-screws (M1.4) above the cerebellum served as ground and reference electrodes. Following a one-week postoperative recovery period, the tetrodes were lowered into the CA1 or CA3 regions of the hippocampus (close to the *stratum pyramidale*) over a further period of around 7 days. Wide-band (0.1Hz–5 kHz) recordings

Nature Neuroscience: doi:10.1038/nn.2599

of local field potentials (LFPs) and multiple-unit activity were amplified 1,000-fold via a 64-channel Sensorium amplifier (Charlotte, VT, USA) and continuously digitized at 20 kHz using a 64-channel analogue-to-digital converter computer card (United Electronics Industries, Canton, MA, USA). Two 32-channel unity-gain preamplifier headstages (Axona Ltd, St Albans, Hertfordshire, UK) were used to reduce cable movement artefacts. A small array of three light-emitting diode clusters mounted on the preamplifier headstages was used to track the location of the animal (25 frames per s) *via* an overhead video camera (Sony, Japan). The animal tracking was synchronized with the electrophysiological recording. The animal's location was constantly monitored throughout the daily experiment. The data were analyzed off-line. Analysis programs were written in C programming and Shell scripting languages and run under LINUX (Fedora core 10, http://fedoraproject.org/) operating in an XWindow environment. Statistical analyses were performed using custom made software, including all unit isolation and field analysis, and, occasionally the STAT 5.4 UNIX software package [3] and the R software environment (http://www.r-project.org/).

Apparatus. The behavioral apparatus used for these experiments (see **Supplementary Fig. 1a**) was a circular arena referred to as the cheeseboard maze [4,5]. The board (120 cm in diameter, 2 cm in thickness) was made in plastic, painted black and stood 55 cm above the floor in the recording room (Courtesy of Mr. Philippe Lalanne and Mr. Frédéric Dussutour, Lycee Val de Garonne, Marmande, France). A total of 177 food wells (2.5 cm in diameter, 1.5 cm in depth) were drilled into the surface of the maze in evenly spaced parallel rows and columns (8 cm between the centers of each well). A wood-made black start-box (27 cm long, 19 cm wide and 59 cm high) was placed along the edge of the board perpendicular to

Nature Neuroscience: doi:10.1038/nn.2599

the rows of food wells. The top of the box was open to allow tracking the animal inside; the floor covered by a brown card box and the front equipped with a door (35 cm high). A small glass-made cup (2.5 cm in diameter) was placed inside the start-box.

Experimental procedure

Training. Altogether seven rats were trained to perform the retrieval of the hidden rewards task on the cheeseboard maze. Behavioral training was performed after electrodes implantation during days when the electrodes were moved towards the hippocampus, but before they reached the hippocampus. Following the postoperative recovery period, rats were reduced to and maintained at 85% of their age-matched preoperative weight. Water was available *ad libitum*. Each animal was handled and familiarized with both the testing apparatus in the recording room and the general procedure before data acquisition. First, the rat was allowed to freely explore the whole apparatus for at least 30 min during 3 days. Then, the rat was trained to chase for food-rewards and come back to the start-box. Three groups of visible food pellets (MLab rodent tablet 45mg, TestDiet) were spread out on the surface of the cheeseboard maze while the rat was inside the start box. For each trial, the door was temporarily opened, the animal was allowed to exit the box and retrieve all the rewards while another additional reward was placed in the glass-made cup situated within the start-box. Once all the rewards had been collected, the door was re-opened and the rat was gently conducted back to the start box to find and consume the additional food reward within the start box. That procedure was repeated until the rat started to return back consistently on its own after having collected all the rewards within the board (~3-4 days). A similar procedure was applied over the following days, this time with three hidden rewards (i.e., one food pellet per baited location) within the cheeseboard maze (~2-3 days).

Nature Neuroscience: doi:10.1038/nn.2599

To prevent the use of an odor-guided search strategy during these experiments, food pellet dust was scattered across the maze before each experiment, the board was periodically wiped (using the towel used to handle the rat daily) and the board was rotated relative to the start-box between learning trials and between rest and probe sessions. This initial phase of the experiment ended when the rat was familiar with the whole procedure.

Four of the seven rats trained to perform the hidden rewards task were also trained to retrieve food rewards from visually marked locations ("Cued condition"). To do so, three identical objects (Falcon tube 50 ml, Greiner, see **Supplementary Fig. 1a**) were placed near the baited food-wells during the learning trials and rats were trained to retrieve the hidden rewards from those visually marked locations. In this circumstance, the task was solved by using a guidance strategy that consisted of moving towards intra-maze cues identified to be closely associated with the goals. These intra-maze cues were removed for the two probe tests. This cued training was performed once rats were trained to the hidden rewards task but before the recording sessions started.

Testing. Each daily experiment consisted of a sequence of five recording sessions in the following order: a probe test ("pre-probe"), an immobility/sleep rest session ("pre-rest"), a learning session, an immobility/sleep rest session ("post-rest") and a probe test ("post-probe") (see **Supplementary Fig. 1b**). The two probe tests (~25 min) were never rewarded. After both the pre-probe and the learning sessions, rats were allowed to settle down within the start box for the rest sessions (~25 min). During the learning session, rats were given successive trials (~40 trials) to find the 3 hidden rewards placed in randomly selected food-wells. As these baited locations changed from day-to-day but stayed fixed within a given day, this matching-to-multiple-places procedure required frequent updating of memory for goal locations in an otherwise unchanging environment. The same paradigm was used for

Nature Neuroscience: doi:10.1038/nn.2599

the NMDAR blockade experiments during which rats were injected with the 3-((R)-2-Carboxypiperazin-4-yl)-propyl-1-phosphonic acid [(R)-CPP, 10mg.kg^{-1} i.p., Tocris Cookson Ltd, Bristol, UK] after the pre-probe session [6-9]. In this condition, the learning session started 1.5h after the CPP injection to ensure that NMDARs were blocked before starting the subsequent learning session [7].

Subjects. In all a total of 12 (from 6 animals), 8 (from 3 animals) and 9 (from 4 animals) sequences of probe-rest-learning-rest-probe recorded in the familiar recording room were analyzed for the drug-free, CPP and Cued conditions respectively. In three animals were recorded all 3 experimental conditions, each in different consecutive days, starting with the visually-guided task ("Cued condition", 1-2 days), followed by the hidden rewards task ("drug-free condition", 1-3 days) and finally the hidden rewards task in which CPP was applied ("CPP condition", 1-3 days). In one animal recordings were performed in the cued condition only because the quality of unit recordings deteriorated before recordings could be performed in the two other conditions. After completion of the experiments, the rats were deeply anesthetized and perfused through the heart with 0.9% saline solution followed by a 4% buffered formalin phosphate solution for the histological verification of the electrode tracks.

Data analysis

Unit isolation and selection. Unit isolation and clustering procedures have been described previously [1,10,11]. Briefly, the continuously recorded wide-band signals were digitally high-pass filtered (0.8–5 kHz). The power (root mean square) of the filtered signal was computed in a sliding window (0.2 ms) for spike detection. The standard deviation (SD)

Nature Neuroscience: doi:10.1038/nn.2599

was calculated to estimate the variance of the baseline noise and to establish a detection threshold. Action potentials with a power of more than five times the SD from the baseline mean were selected. The spike features were then extracted by using principal components analyses. The detected action potentials were then segregated into putative multiple single units by using automatic clustering software [12] (http://klustakwik.sourceforge.net/). Finally, the generated clusters were manually refined by a graphical cluster cutting program [10]. Only units with clear refractory periods (<2ms) in their autocorrelation and well-defined cluster boundaries [12] were used for further analysis. Pyramidal cells and interneurons were discriminated by their autocorrelations, firing rates and wave forms, as previously described [11]. Because our goal was to analyze changes in the firing patterns of pyramidal cell ensembles over different time points, we needed to ensure that our sample of cells was taken from clusters with stable firing. We therefore clustered together periods of waking spatial behavior and rest sessions. Stability of the recorded cells over time was verified by plotting spike features over time and by plotting 2-dimensional unit cluster plots in different sessions in addition to the stability of spike waveforms. In addition, an isolation distance based on Mahabalonis distance was calculated to ensure that the selected spike clusters did not overlap during the course of the recordings [12]. In total, 2040 CA1 pyramidal cells (drug-free=1074, CPP=612, cued=354) and 690 CA3 pyramidal cells (drug-free=257, CPP=221, cued=212) were included in the analysis.

Definition of exploration and immobility/sleep periods. Recordings sessions were segregated off-line onto periods of exploratory activity and rest (immobility/sleep) as previously described [1,10,11]. For each session, the theta/delta ratio was plotted against speed so that the behavioral state could be manually identified. The theta/delta power ratio was measured in 1600 ms segments (800 ms steps between measurement windows), using Thomson's multi-taper method [13,14]. Exploratory epochs included periods of locomotion

Nature Neuroscience: doi:10.1038/nn.2599

and/or the presence of theta oscillations (as seen in the theta/delta ratio), with no more than 2.4 seconds (i.e., two consecutive windows) of transient immobility. Rest epochs were selected when both the speed and theta-delta ratio dropped below a pre-set threshold (speed: <5cm/s, theta/delta ratio: <2) for at least 2.4 seconds.

Field detection. Both theta and SWRs detection were performed as previously described [1,11]. For the detection of theta-oscillatory waves, the local field potential was filtered (5–28 Hz) and the negative peaks of individual theta waves were detected. For the detection of SWRs, local field potentials were band-pass filtered (150–250 Hz), and a reference signal (from a channel that did not contain ripple oscillations) was subtracted to eliminate common-mode noise (such as muscle artefacts). The power (root mean square) of the filtered signal was calculated for each electrode and summed across electrodes designated as being in the CA1 pyramidal cell layer. The threshold for SWR detection was set to 7 SD above the background mean. The SWRs detection threshold was always set in the first immobility/sleep session, and the same threshold was used for all other sessions. SWRs detected during exploration were designated eSWRs, and those during immobility/sleep rest periods as sSWRs [1,2].

Nature Neuroscience: doi:10.1038/nn.2599

3. Supplementary Figures

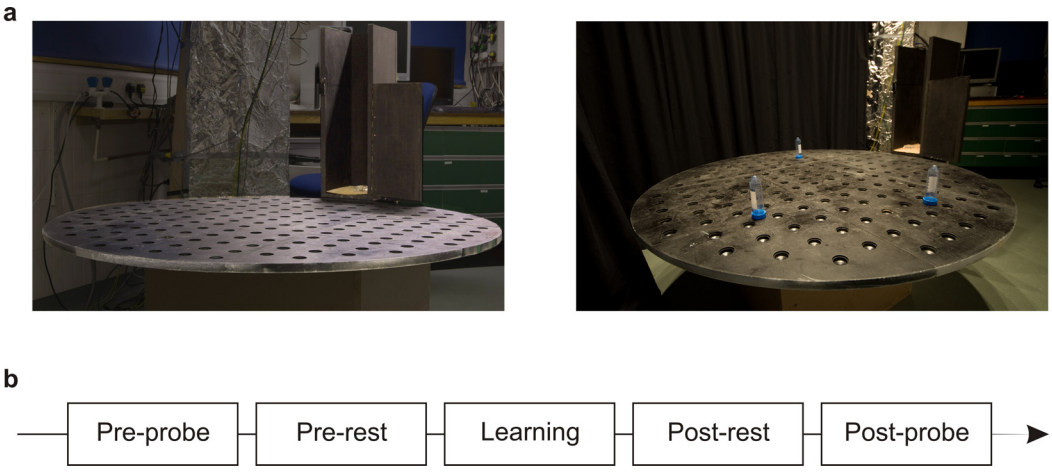

Supplementary Figure 1. Experimental set up and behavioral procedure

(a) Behavioral apparatus including the cheeseboard maze and the connected start-box without (*left*, Drug-free and CPP conditions) or with (*right*, Cued condition) the intra-maze cue objects.

(b) Behavioral procedure including two unrewarded probe sessions and one learning session bracketed by two immobility/sleep rest sessions (marked as "pre-rest" and "post-rest"). Each recording day began with the "pre-probe" and ended with the "post-probe" which tested memory for old goal locations (learnt the previous day) and newly-learnt goal locations respectively.

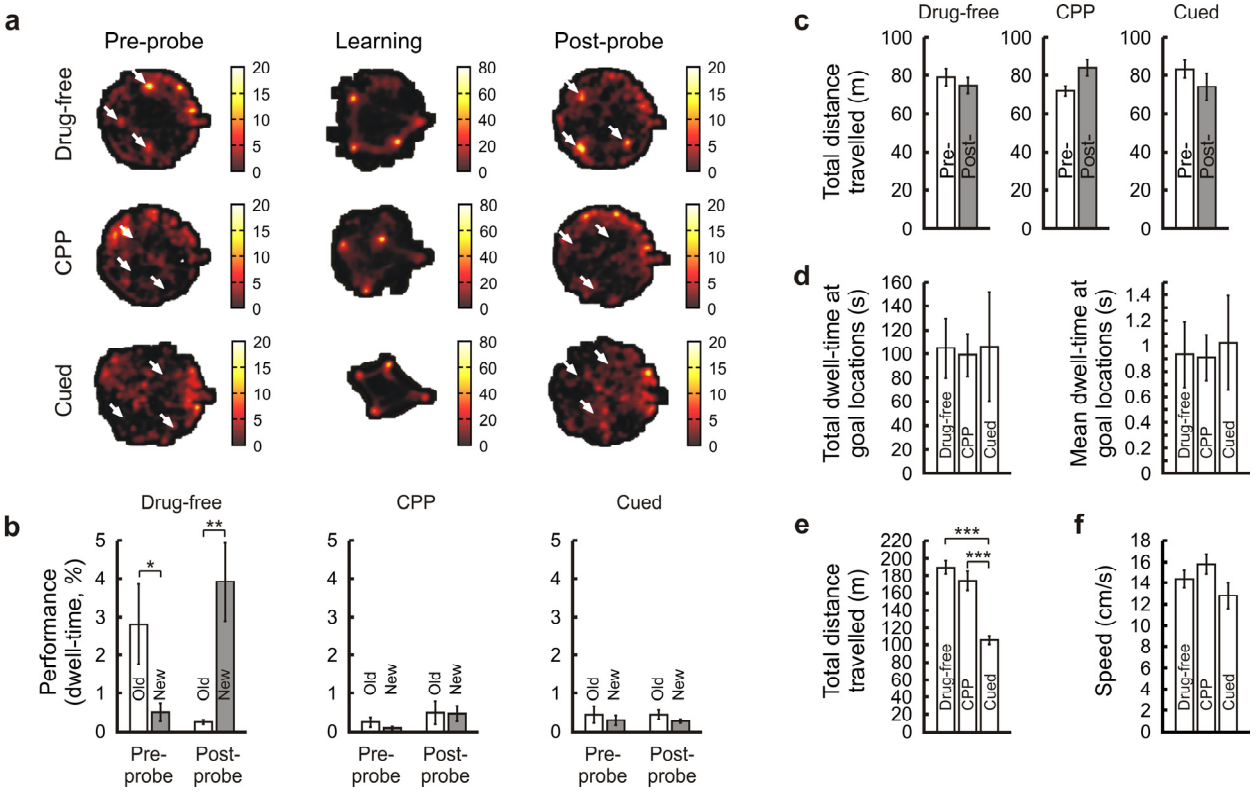

Supplementary Figure 2. Quantification of the behavior in the cheeseboard maze

(a) Representative examples of occupancy maps (z scale=time in sec) on the cheeseboard maze during the probe and the learning (40 trials) sessions from all three conditions. The white arrows in the pre-probe and the post-probe maps indicate the old goal locations (learnt the previous day) and the newly-learnt goal locations respectively.

(b) Memory retention performance during the probe sessions as estimated by the percentage of dwell-time at goal areas (means±s.e.m, see Methods) from rats in the drug-free (*left*), CPP (*middle*) and Cued (*right*) conditions. Dwell-times were compared for goal locations learnt the day before ("Old") and the current day ("New"). Note that rats in the drug-free condition spent more time at the newly-learnt bait-locations than the old ones learnt the day before (post-probe: P=0.0019) and that these locations were also remembered on the following day, as assessed during the pre-probe session of the next day (pre-probe: P=0.034). This was neither the case under CPP (all Ps>0.296) nor in the cued condition (all Ps>0.209). *: P<0.05, **: P<0.01, paired t-test.

(c) Total distance travelled (means±s.e.m) during the probe sessions by rats in the drug-free (*left*), the CPP (*middle*) and the Cued (*right*) condition (all Ps>0.091, paired t-test). Pre-= pre-probe, Post-= post-probe.

(d) Dwell-time at goal locations during learning (means±s.e.m; *left*: dwell-time at goal locations for the entire session; *right*: average dwell-time per goal location per learning trial) from rats in all three conditions. Note that rats in all three conditions spent similar amount of time at the goal locations (all Ps>0.953, ANOVA).

(e) Total distance travelled during learning trials from rats in all three conditions (means±s.e.m, P<0.000001, ANOVA). Note that rats in the two un-cued goal locations conditions (drug-free and CPP) travelled similar path length from leaving the start-box to returning (P>0.373, Tukey's HSD post-hoc) but travelled longer path length compared with the Cued condition (all Ps<0.0001, Tukey's HSD post-hoc). This is explained by the longer distance travelled to find the goal locations during the first trials (see **Figure 1a** and **Figure 3a**).

(f) Animals speed during learning trials from rat in all three conditions (means±s.e.m, P>0.130, ANOVA).

Nature Neuroscience: doi:10.1038/nn.2599

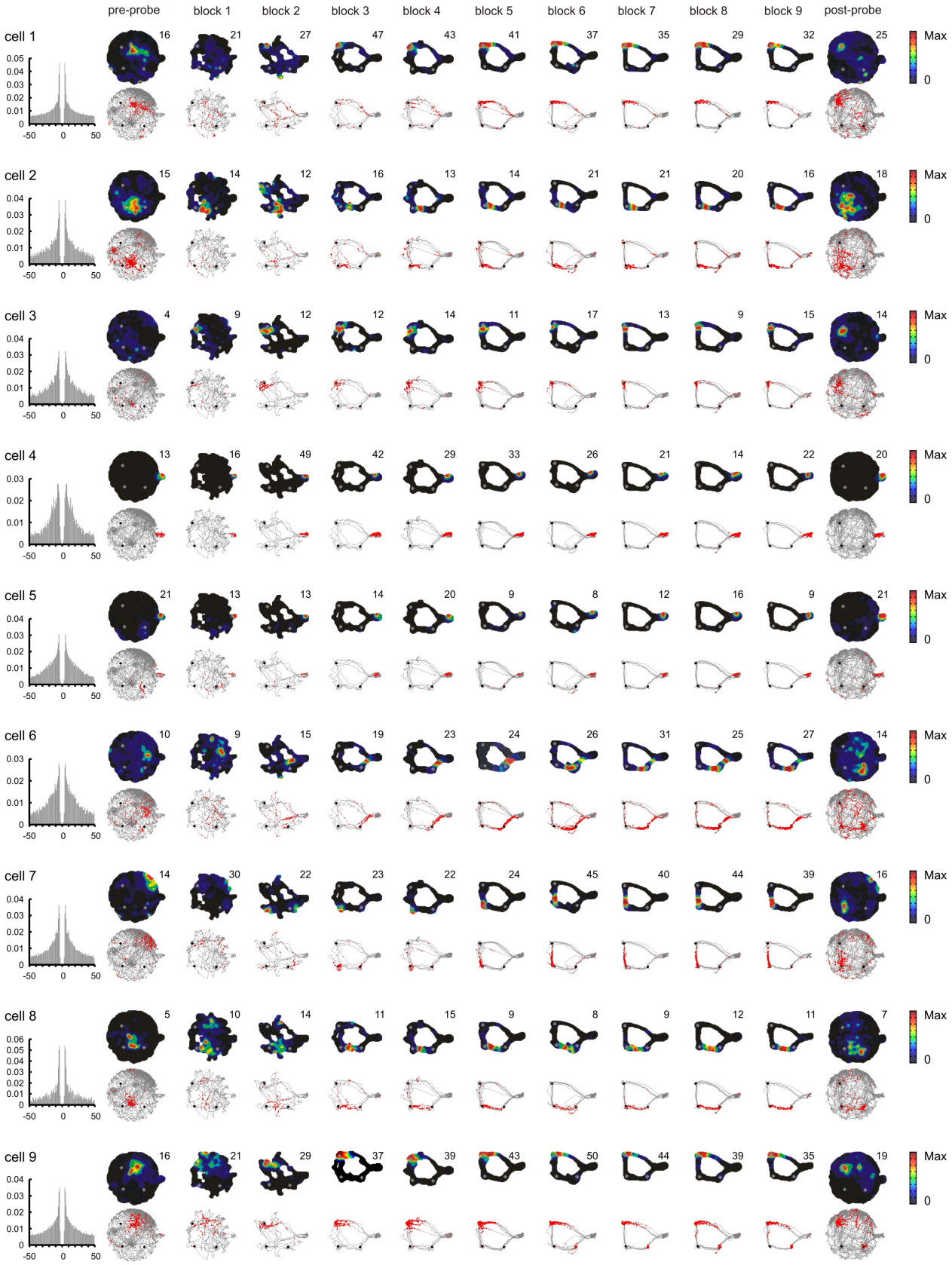

Nature Neuroscience: doi:10.1038/nn.2599

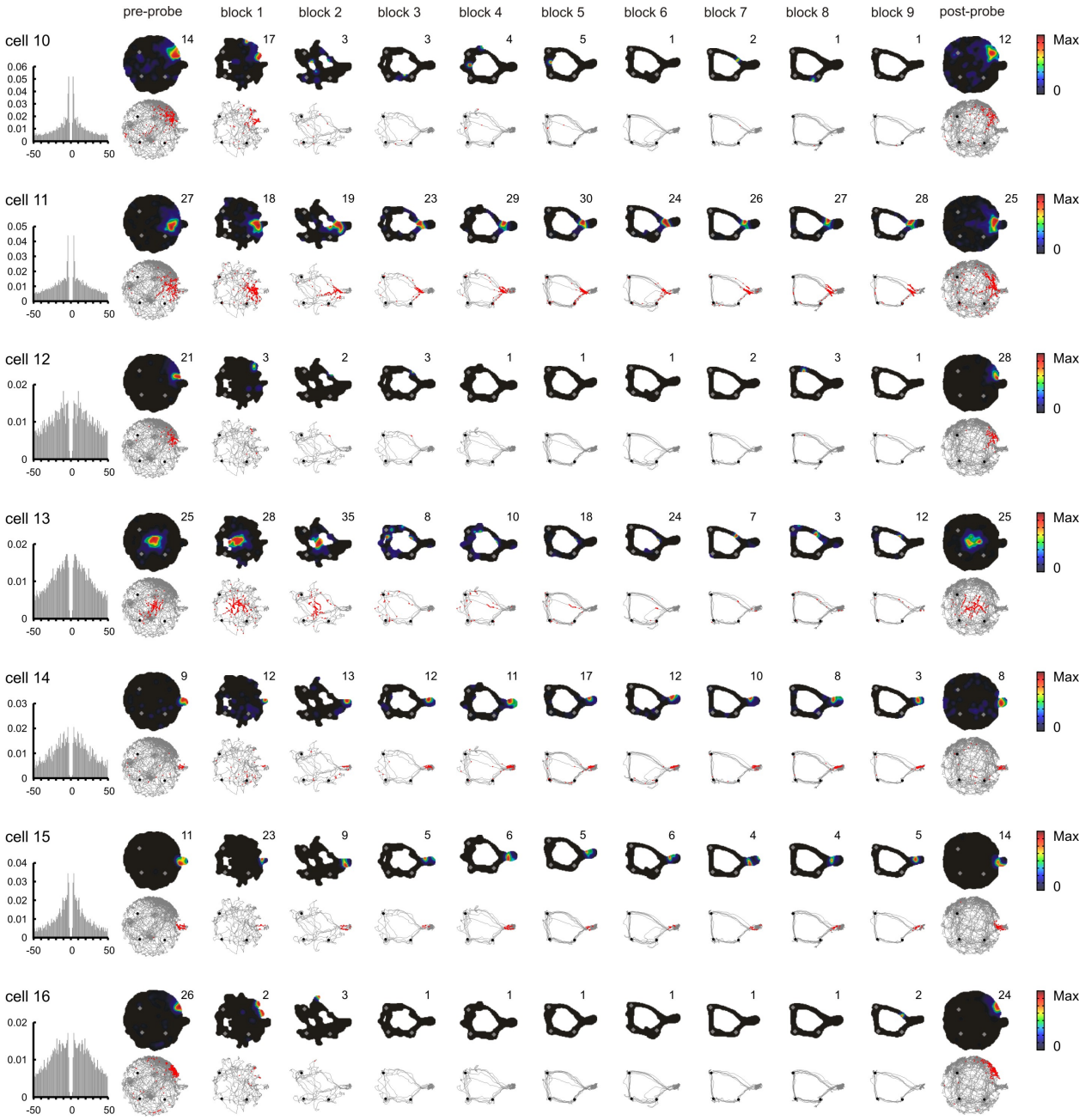

Supplementary Figure 3. Examples of CA1 and CA3 hippocampal place cells recorded in the drug-free condition

Simultaneously recorded place cells from the CA1 (cells 1–11) and CA3 (cells 12–16) regions of the hippocampus are shown on alternating rows with auto-correlogram, color-coded place rate maps and individual spike locations superimposed on the animal's path. Both rate maps and raw spike data are depicted for each probe session ("pre-probe", "post-

Nature Neuroscience: doi:10.1038/nn.2599

probe") and across successive learning trial blocks. The first block represented the first learning trial only while the rest of the blocks consisted of 5 consecutive trials. The color code in the rate maps is from blue (low firing rate) to red (peak firing rate), with the maximum firing rate (Hz) of the color scale indicated on the top right of each map. High firing rate regions marked by warm colors indicate the "place field" of the cell and gray dots indicate the goal locations. Red dots mark locations where the cell fired action potentials while gray traces show animal movement path and black dots indicate the goal locations. Note that some CA1 place cells (cells 1–3,6–9) reorganize to represent the goal locations while some do not (cells 4,5,10,11). Note the stable place fields of CA3 place cells across behavioral sessions (cells 12–16).

Nature Neuroscience: doi:10.1038/nn.2599

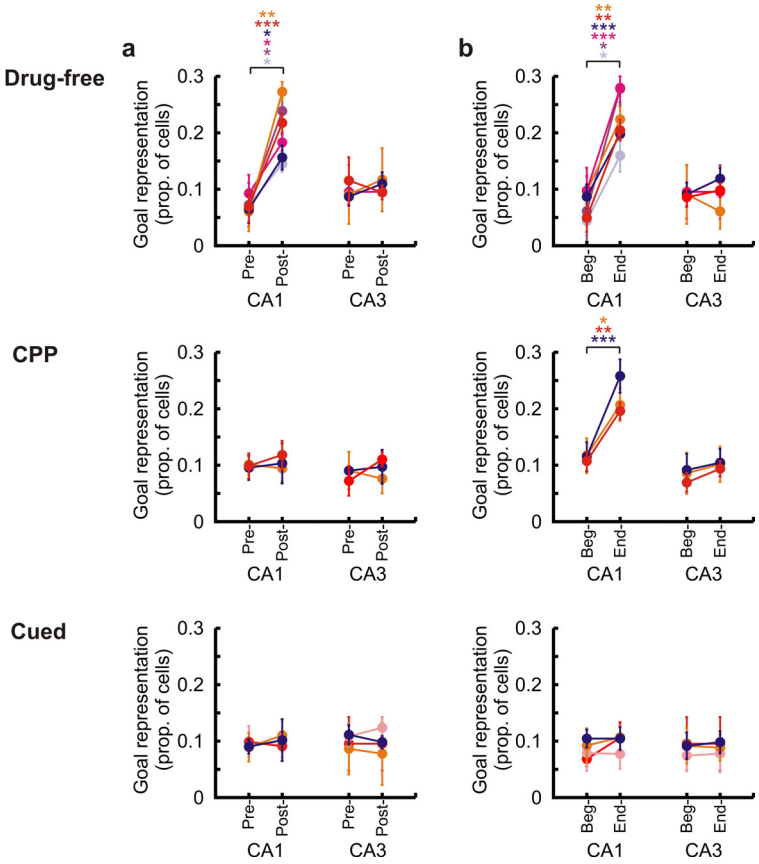

Supplementary Figure 4. Hippocampal place cell representation of goal locations for individual animals in the drug-free, CPP and Cued conditions

Proportion of place cells representing bait-locations (means±s.e.m) in the CA1 and CA3 regions of the hippocampus during the probe sessions (**a**, Pre-= pre-probe, Post-= post-probe) and during the learning session (**b**, Beg-= beginning of learning, End-= end of learning) for individual animals. In these panels, goal representation was estimated by the proportion of cells with a place field centre falling within 10cm from the center of a baited well (see Methods). *: P<0.05, **: P<0.01, ***: P<0.001, paired t-test.

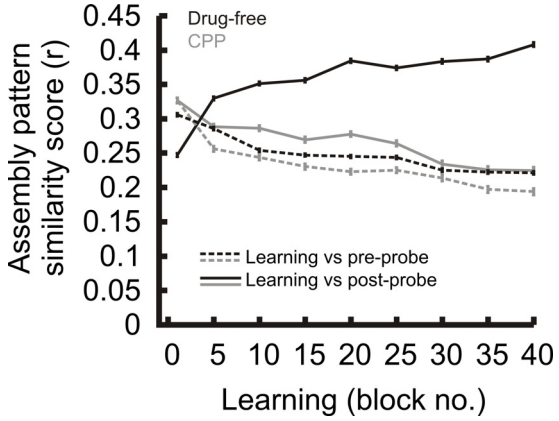

Supplementary Figure 5. Reorganization of CA1 assembly patterns during learning

Assembly patterns similarity score (means±s.e.m.) determined over the course of learning using a population vector analysis [15,16] (see Methods). In the drug-free condition (black lines), CA1 assembly patterns became gradually more similar to assembly patterns present in the probe session after learning ("post-probe", solid black line) and more dissimilar to assembly patterns present in the probe session before learning ("pre-probe", dashed black line) (all Ps<0.00001, ANOVA). This explains why CA1 assembly patterns at the end of learning (i.e., the last 10 trials) were more similar to post-probe than pre-probe assembly patterns (see Drug-free in **Figure 2g**). In the CPP condition (grey lines), CA1 assembly patterns became gradually more dissimilar to the pre-probe assembly patterns (dashed grey line) but also to the post-probe assembly patterns (solid grey line) (all Ps<0.00001, ANOVA). This decreased similarity with the post-probe reflects a decreased ability to subsequently recall CA1 representations gradually-established during learning (see CPP in **Figure 2d**), and therefore highlights the impaired stabilization of the reorganized CA1 place maps (see CPP in **Figure 2c**) and the fact that the probe representations remained unchanged by learning (see CPP in **Figure 2f**).

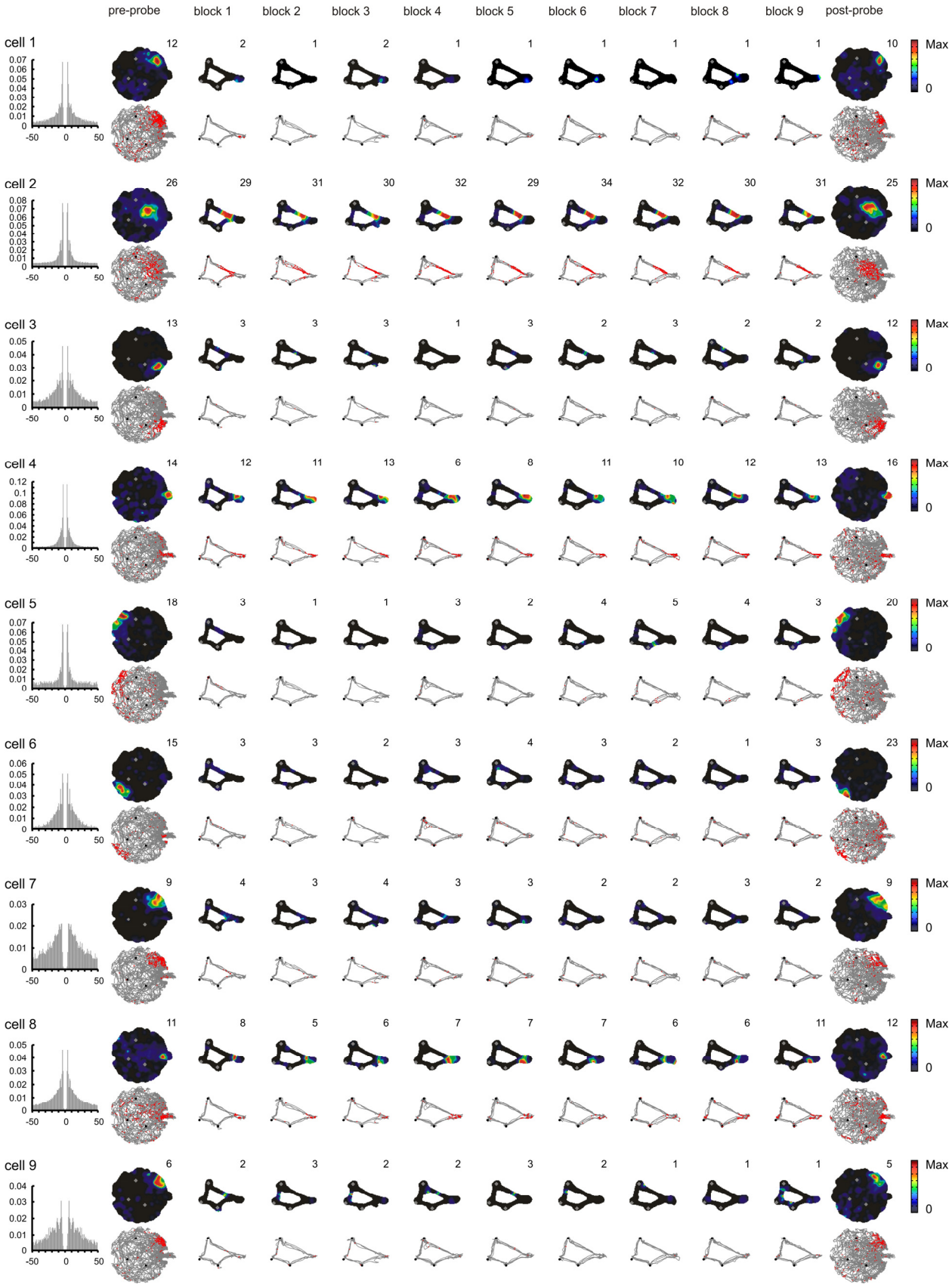

Nature Neuroscience: doi:10.1038/nn.2599

Supplementary Figure 6. Examples of CA1 hippocampal place cells recorded in the Cued condition

Simultaneously recorded place cells from the CA1 region of the hippocampus in the cued version of the task are shown on alternating rows with auto-correlogram, color-coded place rate maps and individual spike locations superimposed on the animal's path. Both rate maps and raw spike data are depicted for each probe session ("pre-probe", "post-probe") and across successive learning trial blocks. The color code in the rate maps is from blue (low firing rate) to red (peak firing rate), with the maximum firing rate (Hz) of the color scale indicated on the top right of each map. High firing rate regions marked by warm colors indicate the "place field" of the cell and gray dots indicate the goal locations. Red dots mark locations where the cell fired action potentials while gray traces show animal movement path and black dots indicate the goal locations. Note that CA1 place maps remained unchanged by the cued learning.

Nature Neuroscience: doi:10.1038/nn.2599

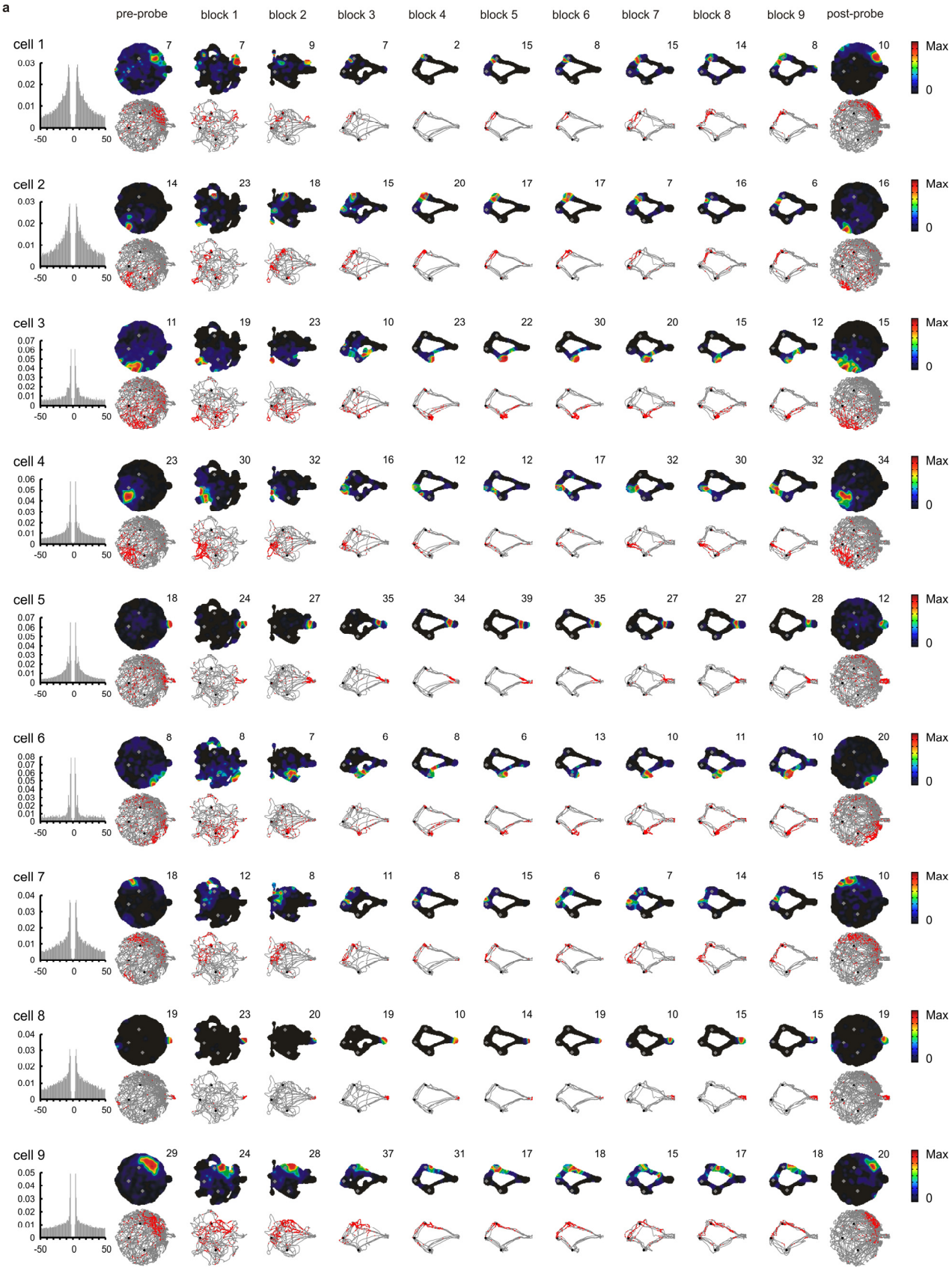

Nature Neuroscience: doi:10.1038/nn.2599

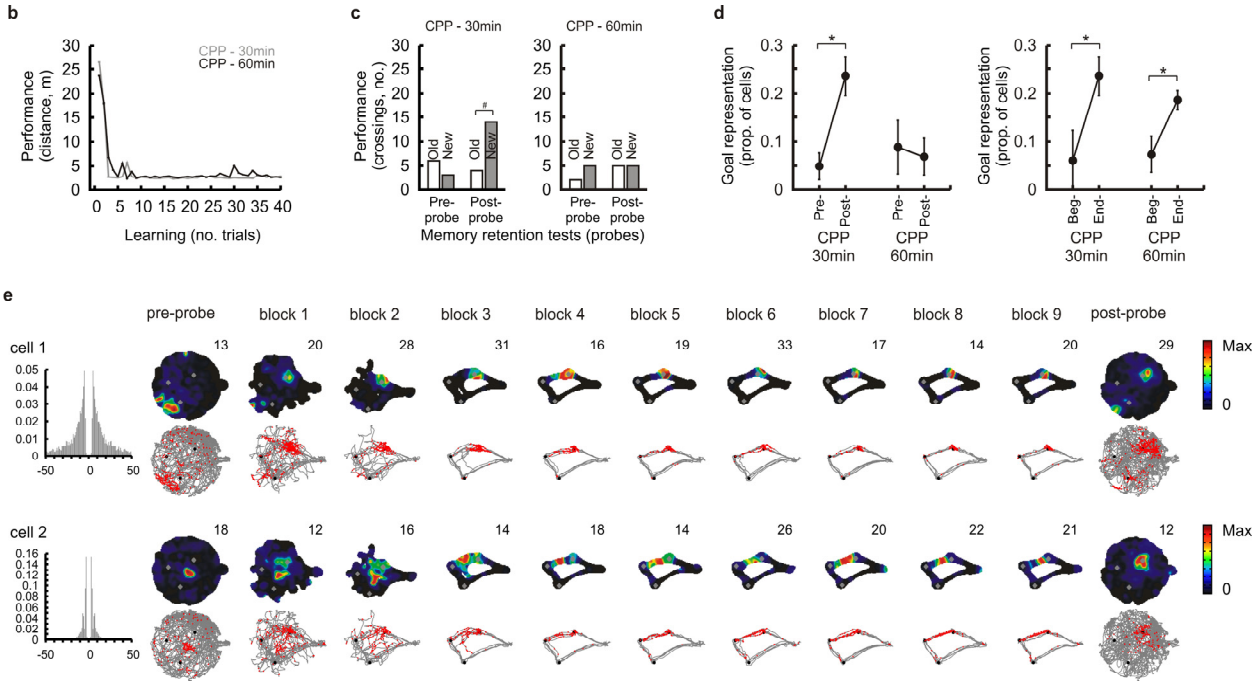

Supplementary Figure 7. CA1 hippocampal place maps in the CPP condition

(a) Examples of simultaneously recorded place cells from the CA1 region of the hippocampus under CPP are shown on alternating rows with auto-correlogram, color-coded place rate maps and individual spike locations superimposed on the animal's path. Both rate maps and raw spike data are depicted for each probe session ("pre-probe", "post-probe") and across successive learning trial blocks. The color code in the rate maps is from blue (low firing rate) to red (peak firing rate), with the maximum firing rate (Hz) of the color scale indicated on the top right of each map. High firing rate regions marked by warm colors indicate the "place field" of the cell and gray dots indicate the goal locations. Red dots mark locations where the cell fired action potentials while gray traces show animal movement path and black dots indicate the goal locations. Note that under CPP many CA1 place cells reorganized to represent the goal locations during the learning period. However, place maps in the post-probe session reverted back to that observed during the pre-probe session (cells 1–4,6,7,9).

(b-e) Memory performance and place maps after 30 and 60min post-learning delay in the CPP condition. One additional rat was trained to locate the 3 hidden food-rewards on the cheeseboard maze in the CPP condition (see Methods) with the post-probe test performed either 30 minutes ("CPP-30min") or 60 minutes ("CPP-60min") after the end of the learning period. Behavioral performance are shown during the learning period (**b**, distance travelled to find all 3 hidden rewards per trial) and during the memory retention tests (**c**, number of crossings in goal areas). Crossings were compared for goal locations learned the

day before ("Old") and the current day ("New"). Note that the CPP-treated animal remembered the newly-learnt goal locations after 30min but not after 60 minutes ($^{\#}$: $P<0.05$, binomial test). In these experiments, the proportion of CA1 place cells representing bait-locations was quantified (**d**, means±s.e.m) during the probe sessions (Pre-: pre-probe, Post-: post-probe) and during the learning session (Beg-: beginning of learning, End-: end of learning). Note that under CPP the CA1 representation of the goal locations reemerged during the post-probe session when performed 30 minutes after the end of the learning (*: $P<0.05$, paired t-test). Examples of CA1 place cells recorded in the "CPP-30min" condition are shown on alternating rows with auto-correlogram, color-coded place rate maps and individual spike locations superimposed on the animal's path (**e** shown as in panel **a**). Note that, in this condition, CA1 place cells that reorganized to represent the goal locations during learning still represent those locations during the post-probe after 30 min post-learning delay in association with good memory retention performance (**c**).

Nature Neuroscience: doi:10.1038/nn.2599

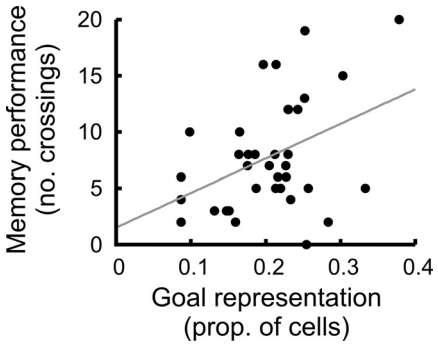

Supplementary Figure 8. Scatter plot showing the post-probe memory performance (number of crossings) as a function of the proportion of CA1 place cells representing the new goal locations in the probe session after learning (in grey: regression line, r=0.405, P=0.014).

Nature Neuroscience: doi:10.1038/nn.2599

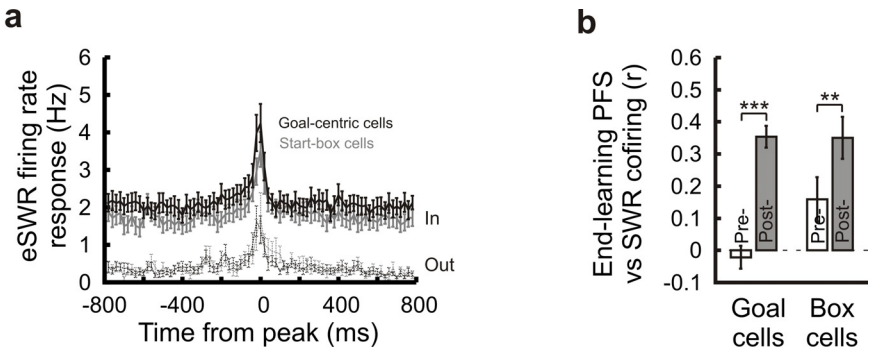

Supplementary Figure 9. SWR responses of CA1 place cells in the Cued version of the cheeseboard maze task

(a) eSWR firing rate histograms (means±s.e.m) of CA1 "goal-centric" and "start-box" place cells inside ("In") and outside ("Out") their place fields (see Methods).

(b) Correlation between place field similarity ("PFS") and sSWR for "goal-centric" and "start-box" cell pairs (means±s.e.m). The PFS was measured based on place fields established at the end of learning while sSWR cofiring was calculated in rest periods before ("Pre-") and after ("Post-") the learning session (see Methods). Correlation coefficients represent the partial correlations of the PFS with the cofiring of one rest session, each controlled by the cofiring of the other rest session (see Methods). **: $P<0.01$, ***: $P<0.001$, paired t-test.

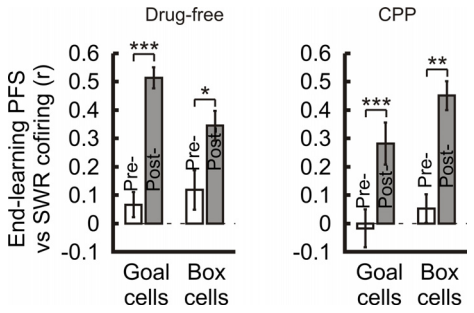

Supplementary Figure 10. Reactivation of CA1 place-related assembly patterns

Correlation between place field similarity ("PFS") and sSWR cofiring calculated for "goal-centric" and "start-box" cell pairs (means±s.e.m). The PFS was calculated based on place fields established at the end of learning while sSWR cofiring was calculated in rest periods before ("Pre-") and after ("Post-") the learning session (see Methods). Correlation coefficients represent the partial correlations of the PFS with the cofiring of one rest session, each controlled by the cofiring of the other rest session (see Methods). Correlation coefficients were calculated separately for each recording session and averaged. *: $P<0.05$, **: $P<0.01$, ***: $P<0.001$, paired t-test.

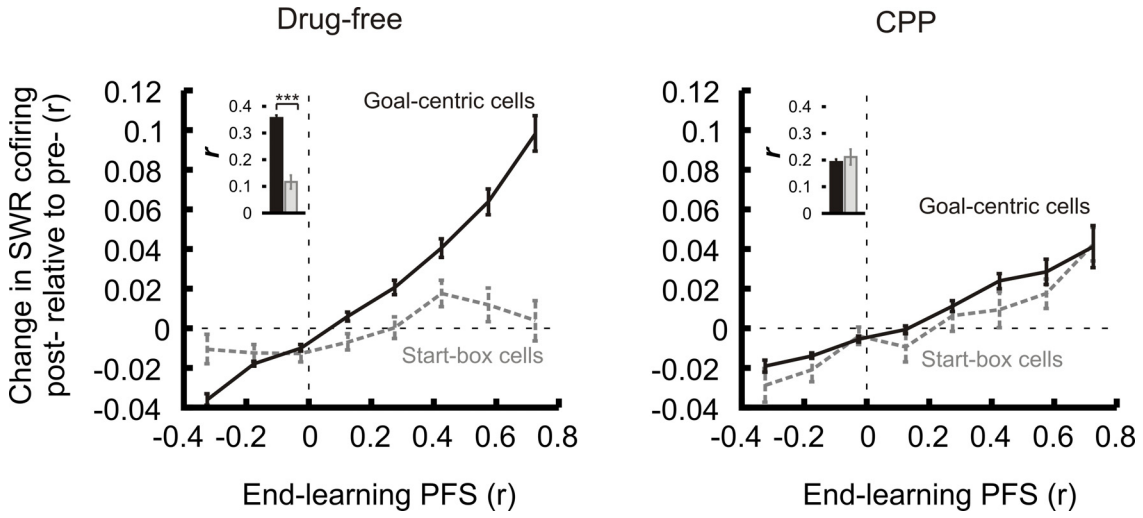

Supplementary Figure 11. Learning-related PFS predicts change in sSWR cofiring

Change in sSWR cofiring from the rest session before learning ("pre-") to the rest session after learning ("post-") as a function of place field similarity ("PFS") measured at the end of learning (means±s.e.m.). Both "goal-centric" and "start-box" cell pairs are shown. Note that for the "goal-centric" cells, both positive and negative changes in sSWR cofiring were observed in all conditions but the strong increase in cofiring observed amongst overlapping "goal-centric" cells was prevented under CPP. Note the steeper slope of the curve for the "goal-centric" cells in the drug-free condition. The inserts show the regression coefficient (means±s.e.m). These results indicate that the reorganization of goal-related patterns needed for reactivation was established during waking experience as a result of NMDAR-dependent changes in cell firing associations. ***: $P<0.001$, paired t-test.

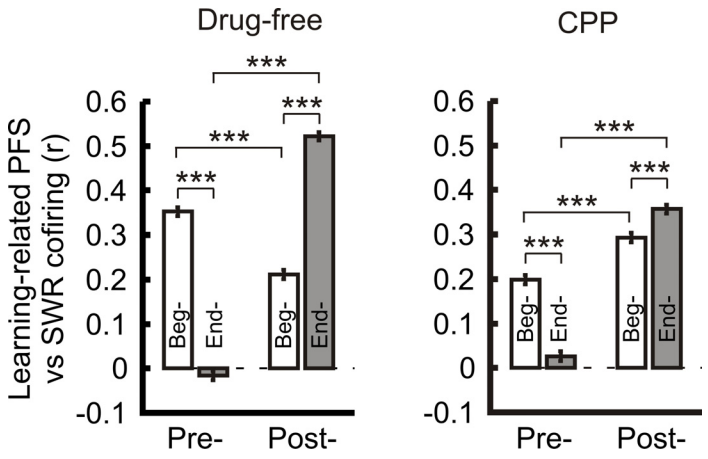

Supplementary Figure 12. Off-line reactivation of conflicting representations under NMDAR blockade

Correlation between the place field similarity ("PFS") calculated from either the beginning ("Beg-") or the end ("End-") of learning and sSWR cofiring during the rest session before learning ("Pre-") and the rest session after learning ("Post-") for cell pairs representing goal locations (means±s.e.m, ***: P<0.001, paired t-test). Correlation coefficients represent the partial correlations of the PFS with the cofiring of one rest session, each controlled by the cofiring of the other rest session (see Methods). Note that the beginning and the end of learning patterns are both reactivated during the post-rest session in the CPP condition (interaction Drug-free/CPP x Beg/End: P=0.0010, ANOVA; CPP/End = CPP/Beg with Tukey's HSD post-hoc).

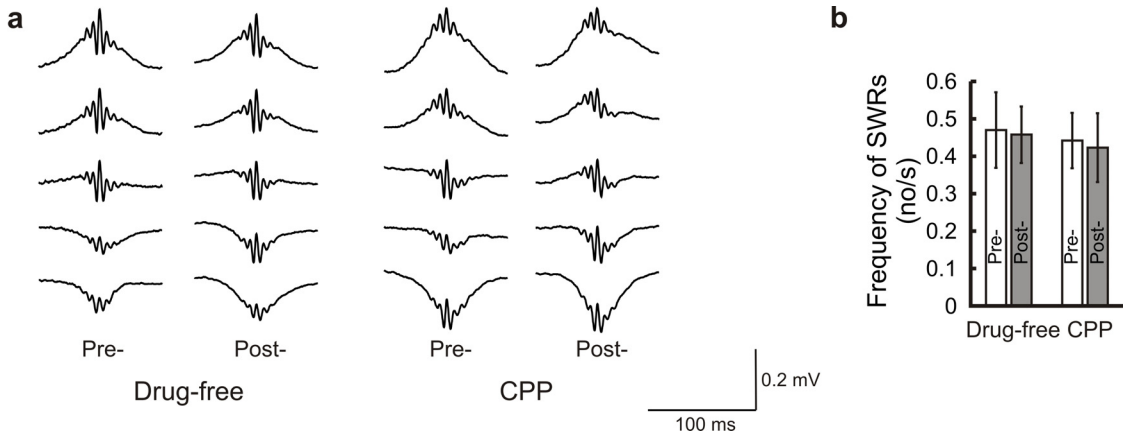

Supplementary Figure 13. SWRs during the rest periods

(a) Traces of averaged sSWRs from the rest session before learning ("Pre-") and the rest session after learning ("Post-") from the same rat in the drug-free and the NMDAR blockade conditions. Note that the average traces are similar.

(b) Occurrence frequency of sSWRs (no./s is the number of sSWRs per sec) during the pre-rest and the post-rest sessions (means±s.e.m, Pre- compared to Post-: all Ps>0.611, paired t-test; group comparison: P>0.985, ANOVA).

4. Supplementary References

1. O'Neill,J., Senior,T. & Csicsvari,J. Place-selective firing of CA1 pyramidal cells during sharp wave/ripple network patterns in exploratory behavior. *Neuron* **49**, 143-155 (2006).

2. O'Neill,J., Senior,T.J., Allen,K., Huxter,J.R. & Csicsvari,J. Reactivation of experience-dependent cell assembly patterns in the hippocampus. *Nat. Neurosci.* **11**, 209-215 (2008).

3. Perlman,G. Data Analysis Programs for the UNIX Operating System. *Behavior Research Methods & Instrumentation* **12**, 554-558 (1980).

4. Kesner,R.P., Farnsworth,G. & Kametani,H. Role of parietal cortex and hippocampus in representing spatial information. *Cereb. Cortex* **1**, 367-373 (1991).

5. Gilbert,P.E., Kesner,R.P. & DeCoteau,W.E. Memory for spatial location: role of the hippocampus in mediating spatial pattern separation. *J. Neurosci.* **18**, 804-810 (1998).

6. Abraham,W.C. & Mason,S.E. Effects of the NMDA receptor/channel antagonists CPP and MK801 on hippocampal field potentials and long-term potentiation in anesthetized rats. *Brain Res.* **462**, 40-46 (1988).

7. Kentros,C. *et al.* Abolition of long-term stability of new hippocampal place cell maps by NMDA receptor blockade. *Science* **280**, 2121-2126 (1998).

8. McDonald,R.J. *et al.* NMDA-receptor blockade by CPP impairs post-training consolidation of a rapidly acquired spatial representation in rat hippocampus. *Eur. J. Neurosci.* **22**, 1201-1213 (2005).

9. Brun,V.H., Ytterbo,K., Morris,R.G., Moser,M.B. & Moser,E.I. Retrograde amnesia for spatial memory induced by NMDA receptor-mediated long-term potentiation. *J Neurosci* **21**, 356-362 (2001).

10. Csicsvari,J., Hirase,H., Czurko,A. & Buzsaki,G. Reliability and state dependence of pyramidal cell-interneuron synapses in the hippocampus: an ensemble approach in the behaving rat. *Neuron* **21**, 179-189 (1998).

11. Csicsvari,J., Hirase,H., Czurko,A., Mamiya,A. & Buzsaki,G. Oscillatory coupling of hippocampal pyramidal cells and interneurons in the behaving Rat. *J. Neurosci.* **19**, 274-287 (1999).

12. Harris,K.D., Hirase,H., Leinekugel,X., Henze,D.A. & Buzsaki,G. Temporal interaction between single spikes and complex spike bursts in hippocampal pyramidal cells. *Neuron* **32**, 141-149 (2001).

Nature Neuroscience: doi:10.1038/nn.2599

13. Thomson,D.J. Spectrum estimation and harmonic analysis. *Proc IEEE* **70**, 1055-1096 (1982).

14. Mitra,P.P. & Pesaran,B. Analysis of dynamic brain imaging data. *Biophys. J.* **76**, 691-708 (1999).

15. Leutgeb,S. *et al.* Independent codes for spatial and episodic memory in hippocampal neuronal ensembles. *Science* **309**, 619-623 (2005).

16. Leutgeb,J.K. *et al.* Progressive transformation of hippocampal neuronal representations in "morphed" environments. *Neuron* **48**, 345-358 (2005).

Nature Neuroscience: doi:10.1038/nn.2599